



HAL
open science

A Parameter-Free Method for Estimating the Stator Resistance of a Wound Rotor Synchronous Machine

Peyman Haghgooei, Ehsan Jamshidpour, Adrien Corne, Nouredine Takorabet, Davood Arab Khaburi, Lotfi Baghli, Babak Nahid-Mobarakeh

► **To cite this version:**

Peyman Haghgooei, Ehsan Jamshidpour, Adrien Corne, Nouredine Takorabet, Davood Arab Khaburi, et al.. A Parameter-Free Method for Estimating the Stator Resistance of a Wound Rotor Synchronous Machine. World Electric Vehicle Journal, 2023, 14 (3), pp.65. 10.3390/wevj14030065 . hal-04024661

HAL Id: hal-04024661

<https://hal.univ-lorraine.fr/hal-04024661v1>

Submitted on 11 Mar 2023

HAL is a multi-disciplinary open access archive for the deposit and dissemination of scientific research documents, whether they are published or not. The documents may come from teaching and research institutions in France or abroad, or from public or private research centers.

L'archive ouverte pluridisciplinaire **HAL**, est destinée au dépôt et à la diffusion de documents scientifiques de niveau recherche, publiés ou non, émanant des établissements d'enseignement et de recherche français ou étrangers, des laboratoires publics ou privés.



Distributed under a Creative Commons Attribution 4.0 International License

A Parameter-free Method for Estimating the Stator Resistance of a Wound Rotor Synchronous Machine

Peyman Haghgooei ¹, Ehsan Jamshidpour ¹, Adrien Corne ², Nouredine Takorabet ¹, Davood Arab Khaburi ³, Lotfi Baghli ¹ and Babak Nahid-Mobarakeh ⁴

¹ Université de Lorraine-GREEN; peyman.haghgooei@univ-lorraine.fr; ehsan.jamshidpour@univ-lorraine.fr, noureddine.takorabet@univ-lorraine.fr, Lotfi.baghli@univ-lorraine.fr

² Université Grenoble Alpes; adrien.corne@univ-grenoble-alpes.fr

³ Iran University of Science and Technology; khaburi@iust.ac.ir

⁴ McMaster University; babak.nahid@mcmaster.ca

* Correspondence: ehsan.jamshidpour@univ-lorraine.fr; Tel.: +33 (0)372744380

Abstract: This paper presents a new online method based on low frequency signal injection to estimate the stator resistance of a Wound Rotor Synchronous Machine (WRSM). The proposed estimator provides a parameter-free method for estimating the stator resistance, in which there is no need to know the values of the parameters of the machine model, such as the stator and rotor inductances or the rotor flux linkage. In this method, a low frequency sinusoidal current is injected in the d axis of the stator current to produce a sinusoidal flux in the stator. In this study, it will be shown that the phase difference between the generated sinusoidal flux and the injected sinusoidal current is related to the stator resistance mismatch. Using this phase difference, the stator resistance is estimated. To validate the proposed model-free estimator, simulations are performed with Matlab Simulink and the results are compared with the extended Kalman filter observer. Finally, experimental tests, under different conditions, are performed to estimate the stator resistance of a WRSM.

Keywords: Resistance estimation, Wound Rotor Synchronous Machine (WRSM), Motor parameters, Parameter identification

Nomenclature

ω_c	Cutoff frequency of the LPF
ω_e	Synchronous angular frequency
ψ_s	Stator flux
φ	Phase error produced by LPF
DTC	Direct Torque Control
EKF	Extended Kalman Filter
i_e	Rotor excitation current
i_s	Stator current
L_d	Stator inductance on the d axis
L_q	Stator inductance on the q axis
LPF	Low Pass Filter
M	Mutual inductance between the rotor and the stator

Citation: Haghgooei, P.; Jamshidpour, E.; Corne, A.; Takorabet, N.; Arab Khaburi, D.; Baghli, L.; Nahid-Mobarakeh, B. A Parameter-free Method for Estimating the Stator Resistance of a Wound Rotor Synchronous Machine. *Journal Not Specified* **2023**, *1*, 0. <https://doi.org/>

Received:

Revised:

Accepted:

Published:

Copyright: © 2023 by the authors. Submitted to *Journal Not Specified* for possible open access publication under the terms and conditions of the Creative Commons Attribution (CC BY) license (<https://creativecommons.org/licenses/by/4.0/>).

Mag	Gain error produced by LPF	28
MPC	Model Predictive Control	29
R_s	Stator resistance	30
v_d	Voltages in the d axis	31
v_q	Voltages in the q axis	32
v_s	Stator voltage	33
$WRSM$	Wound Rotor Synchronous Machine	34
$\hat{\psi}_s$	Estimated flux	35
\hat{R}_s	Initial resistance	36
$\tilde{\psi}_s$	Error part of the estimated flux	37
\tilde{R}_s	Error value of the resistance	38

1. Introduction

Synchronous machines are among the most popular types of electrical machines and are increasingly used in various applications. In recent years, many studies have been carried out on modeling, parameters identification, and control methods for this type of machine[1]. The parametric variation of machines with non-linear models is still an important drawback of automatic system controllers [2]. Most of the advanced control methods for synchronous machines are model-based that are dependent on the parameters of the machine. In particular, the stator resistance has a very important role in many advanced control methods such as Direct Torque Control (DTC) [2], Model Predictive Control (MPC) or sensorless control methods [3]. For example, in DTC control method, a mismatch in the stator resistance value may introduce a considerable error in the estimated flux and electromagnetic torque, which can degrade the control performances. Nevertheless, the stator resistance is not always equal to the value given by the manufacturer and it can change due to age, wear, temperature variations, etc. In addition, when the drive system is taken into account, the resistances of the driver and the interface wires are added to the equivalent stator resistance. Thus, for precise control, a stator resistance estimator is needed.

This paper presents a method for estimating the stator resistance without the need for information about the values of the motor parameters (such as d- and q-axis inductances, etc). The proposed estimator is presented after a review of some existing estimation methods.

According to the scientific literature, the stator resistance estimation methods can be divided into three main categories:

1. Direct measurement methods
2. Model-based estimation methods
3. Signal injection-based methods

Direct measurement methods, usually realize under certain conditions, but due to temperature changes and the rest of the system influences, the resistance does not remain constant during the tests therefore they are not an accurate method.

The model-based estimation methods, are generally sensitive to variations in the motor parameters. Consequently, a precise estimation cannot be made if the parameters of the model are not available [4]. Among these methods, the Kalman filter observer [5–7] can be mentioned which is robust towards measurement noises but requires a high amount of computational power due to the complex matrix operations. Other model-based online methods also presented in the literature that can estimate stator resistance and rotor speed simultaneously, such as full-order observers [8], reduced-order observers [9,10] and

model reference adaptive observers [11–17]. The estimators based on Model Reference Adaptive System (MRAS) compare a reference model (with measured variables) and an adjustable model (with estimated states) and according to the error between these two models, the desired variable is estimated. However, these methods are model-based and require the machine parameters to estimate the stator resistance. Another model reference adaptive estimator is also proposed in [18]. This method unlike the classical model-based methods does not require flux calculation, but the stator resistance estimation is performed individually only if the speed is available. A stator resistance estimator based on fuzzy logic controller is also presented in [19] for an induction motor controlled by DTC technique in which the resistance value is updated during operation. Cheng Luo et al. [20] also propose a "phase-shift" based method to compensate the stator resistance for motor drives. They decoupled the resistance estimator from the speed estimator by introducing a coefficient for operating point tracking compensation. In [21], a sensorless control of surface-mounted PMSM with online resistance estimation is proposed. This method uses a sliding mode observer to estimate the stator currents, and assuming the estimated current error is close to zero, a first-order low pass filter is used to estimate the stator resistance. However, this method may not be precise when the initial resistance error is large [22].

The third category of stator resistance estimation methods is based on signal injection. There are some limited studies on DC signal injection [23–25], low-frequency signal injection [26], and high-frequency signal injection [27,28]. In [24] the authors present a signal injection strategy to estimate the machine temperature through the stator resistance estimation of an induction motor. However, the estimator needs a look-up table for different current and temperature values to obtain the voltage drop in the semiconductors that is used in the algorithm. In [25] a DC-signal injection method is proposed. In this method, a DC signal is injected into the three-phase windings of the stator. Then, using a method that includes a high-pass digital filter, a low-pass digital filter, and a sample-and-hold function, the values of the dc components are obtained, and then the stator resistance is estimated. However, extracting the DC components is not easy since the magnitudes of the DC components are much smaller than the fundamental components and the frequency of the fundamental component depends on the rotor speed and hence on the operating point [29]. In the other hand, due to the current limitations of semiconductor devices, dc-signal injection methods cannot be directly applied to the motors larger than 100hp(75kW) [23]. A low-frequency injection-based method for estimating the stator resistance for PMSMs is proposed in [26]; the method is based on injecting a three-level perturbation into i_d and using two algorithms with different convergence speeds. However, this method is completely model-based and sensitive to the model parameters. Also, unstable convergence may occur in the saturation case [30]. High-frequency signal injection methods are mostly used for initial detection of rotor position [31,32] or estimation of the magnetization state [27], rather than for estimation of stator resistance. In these methods, some other problems such as the skin effect and the reactance values (which at high frequencies are more prominent than the resistance value) must be considered in the analysis [25].

In this paper, a new method based on low-frequency signal injection is proposed to estimate the stator resistance. The first advantage of this method is that it does not require machine parameters, which can be applied to the machines even with unknown parameters. Moreover, the variation of the different parameters does not affect the accuracy of the resistance estimation. The second advantage is the simplicity of the implementation, which does not require any complicated process. In the proposed method, a low-frequency sinusoidal current is injected into the d axis of the stator for a short time. This injected signal can produce a sinusoidal variation on the estimated flux of the q axis if there is a mismatch on the stator resistance value. The phase difference between the injected sinusoidal signal and the sinusoidal variation of the estimated flux is related to the initial value of the stator resistance, which allows to adjust and estimate the correct value of the stator resistance. The rest of the paper is structured as follows. The flux estimation is introduced in Section II. In Section III, the effect of stator resistance mismatch on the estimated flux is studied.

The simulation and method explanation is presented in Section IV, and the experimental validations are provided in Section V. Finally, Section VI concludes this article.

2. Flux estimation

With the method proposed in this paper, in order to estimate the stator resistance, the stator flux must first be estimated. In this study, a flux estimator, based on the voltage model, is used as introduced in [33,34]. In this method, the stator flux linkage can be calculated by integrating the back EMF of the stator windings. The stator voltage in $\alpha\beta$ reference frame is described as (1).

$$v_s = R_s i_s + \frac{d\psi_s}{dt} \quad (1)$$

where R_s is the stator resistance and v_s , i_s , and ψ_s , are the voltage, current, and stator flux respectively. The stator flux can be expressed as follows:

$$\psi_s = \int (v_s - R_s i_s) dt \quad (2)$$

The integration in (2) can cause a drift and saturation problems due to the initial condition or dc offset. To avoid this issue, a Low Pass Filter (LPF) can be used instead of a pure integrator. Equation (3) describes the estimated flux in the Laplace transform. where ω_c is the cutoff frequency of the LPF in radians per second.

$$\psi_s = \frac{(v_s - R_s i_s)}{s + \omega_c} \quad (3)$$

Using a LPF can solve the saturation and drift problems, but it also can add an error in the estimated flux. The gain and phase error produced by LPF can be described as (4)[33], where Mag and φ represent the gain and the phase error respectively, and ω_e is the synchronous angular frequency. It can be seen from (4), that there is a gain decrement and a phase delay due to the LPF.

$$\begin{cases} Mag = \frac{|\omega_e|}{\sqrt{\omega_e^2 + \omega_c^2}} \\ \varphi = \frac{\pi}{2} - \tan^{-1}\left(\frac{\omega_e}{\omega_c}\right) \end{cases} \quad (4)$$

Choosing a cutoff frequency close to the operating frequency can decrease the DC offset of the estimated flux, but also introduces phase and magnitude errors. For example, when a cutoff frequency is chosen equal to the synchronous one ($\omega_c = \omega_e$), the ratio of the estimated flux to the actual flux has a magnitude of $\frac{1}{\sqrt{2}}$ with an angle of $\frac{\pi}{4}$. Thus, to reduce phase and magnitude errors, the cutoff frequency can be set as low as possible, but this will reduce the effectiveness of the low-pass filter in filtering out the DC offset that is likely present in the detected currents or voltages. Reference [34] suggests that the cutoff frequency be chosen as a fraction of the rotation frequency, as follows:

$$\omega_c = \frac{|\omega_e|}{k} \quad (5)$$

where k is a constant. In this case, to prevent the time constant of the LPF from being much increased when the motor speed is close to zero, a lower limit must be considered for ω_c . On the other hand, to eliminate the error produced by LPF, a gain and a phase compensator can be used as (6) [34]. This compensator is exactly the inverse of the error introduced in (4). Therefore, the selection of the gain and phase compensators is performed only using the ω_e and ω_c .

$$\begin{cases} G_c = \frac{\sqrt{\omega_e^2 + \omega_c^2}}{|\omega_e|} \\ \varphi_c = \tan^{-1}\left(\frac{\omega_c}{\omega_e}\right) \end{cases} \quad (6)$$

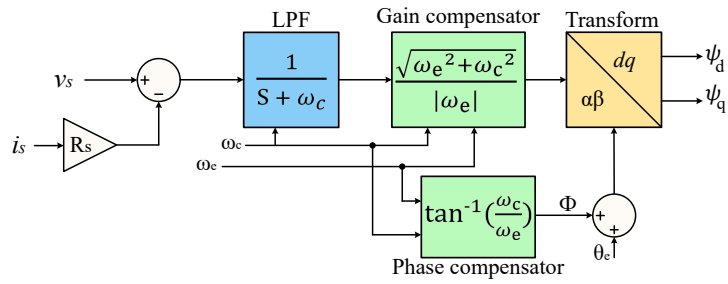


Figure 1. Flux estimation method.

Fig.1 illustrates the block diagram of the flux estimation method. In this method, after the integration of back EMF through an LPF, a gain and a phase compensator is used. Then with a Park transformation, the stator fluxes in dq reference frame are obtained. The stator flux estimator that is introduced, depends on the stator resistance. In the next section, the effect of stator resistance mismatch on flux estimation is investigated.

3. Effect of stator resistance mismatch on the estimated flux

Since the presented flux estimator depends on the stator resistance, it is clear that an error in the stator resistance will cause an error in the estimated flux. By using the difference between the actual flux and the estimated one, the resistance error can be found. However, it is very difficult to measure the actual stator flux and therefore to know the error value of the estimated flux. Thus, in this paper, a method will be proposed to detect the error in the estimated flux without the need to measure the actual flux. Finally using this error, the stator resistance mismatch will be detected.

In order to analyze the effect of stator resistance mismatch on the estimated flux, it is assumed that the compensator performs well, and the result is the same as with a pure integrator as seen in (2).

The resistance error is defines as (7) :

$$\hat{R}_s = R_s + \tilde{R}_s \quad (7)$$

Where R_s is the actual resistance, \hat{R}_s is the initial resistance and \tilde{R}_s is its error value. By substituting (7) in (2), the estimated flux is expressed as (8).

$$\hat{\psi}_s = \int (v_s - (R_s + \tilde{R}_s)i_s)dt = \psi_s + \int -\tilde{R}_s i_s dt \quad (8)$$

Where ψ_s is the actual flux and the rest of the equation is the error part due to the resistance error, the tilde symbol represents the error part as (9).

$$\tilde{\psi}_s = -\tilde{R}_s \int i_s dt \quad (9)$$

If the stator currents in $\alpha\beta$ reference frame are considered sinusoidal as in (10) :

$$\begin{cases} i_\alpha = I_m \cos(\omega_e t) \\ i_\beta = I_m \sin(\omega_e t) \end{cases} \quad (10)$$

By developing (9) and (10), the estimated flux error due to the resistance mismatch can be described as (11) :

$$\begin{cases} \tilde{\psi}_\alpha = \frac{-\tilde{R}_s I_m}{\omega_e} \sin(\omega_e t) \\ \tilde{\psi}_\beta = \frac{\tilde{R}_s I_m}{\omega_e} \cos(\omega_e t) \end{cases} \quad (11)$$

By transforming (11) in dq reference frame, the estimated flux error can be expressed by (12), where \tilde{R}_s is the error value of the stator resistance.

$$\begin{cases} \tilde{\psi}_d = \frac{-\tilde{R}_s I_q}{\omega_e} \\ \tilde{\psi}_q = \frac{\tilde{R}_s I_d}{\omega_e} \end{cases} \quad (12)$$

According to (12), the resistance mismatch can cause an error in the estimated flux. In the field weakening region (i_q positive and i_d negative), it can be noticed from (12) that a positive \tilde{R}_s causes $\tilde{\psi}_d$ and $\tilde{\psi}_q$ to be negative and creating a negative offset in the estimated fluxes $\hat{\psi}_d$ and $\hat{\psi}_q$. Similarly, a negative \tilde{R}_s makes $\tilde{\psi}_d$ and $\tilde{\psi}_q$ positive and therefore it causes to a positive offset for the estimated fluxes $\hat{\psi}_d$ and $\hat{\psi}_q$. This behavior will also be observed in the simulation section.

Another consideration is the effect of stator resistance mismatch on the estimated flux profile in terms of currents. The effect of this mismatch on the flux gradient in terms of currents is shown in (13). In these relations, it is assumed that ($I_{d1} < I_{d2}$ and $I_{q1} < I_{q2}$).

$$\begin{cases} \frac{\Delta\tilde{\psi}_d}{\Delta I_d} |_{I_q=cte} = \frac{\tilde{R}_s I_q (\frac{1}{\omega_{e1}} - \frac{1}{\omega_{e2}})}{I_{d2} - I_{d1}} \xrightarrow{\omega_{e1} > \omega_{e2}} \text{sign}(\frac{\Delta\tilde{\psi}_d}{\Delta I_d}) \propto -\tilde{R}_s \\ \frac{\Delta\tilde{\psi}_q}{\Delta I_q} |_{I_d=cte} = \frac{\tilde{R}_s I_d (\frac{1}{\omega_{e2}} - \frac{1}{\omega_{e1}})}{I_{q2} - I_{q1}} \xrightarrow{\omega_{e2} > \omega_{e1}} \text{sign}(\frac{\Delta\tilde{\psi}_q}{\Delta I_q}) \propto \tilde{R}_s \\ \frac{\Delta\tilde{\psi}_q}{\Delta I_d} |_{I_q=cte} = \frac{\tilde{R}_s (\frac{I_{d2}}{\omega_{e2}} - \frac{I_{d1}}{\omega_{e1}})}{I_{d2} - I_{d1}} \xrightarrow{\omega_{e1} > \omega_{e2}} \text{sign}(\frac{\Delta\tilde{\psi}_q}{\Delta I_d}) \propto \tilde{R}_s \end{cases} \quad (13)$$

According to (13), it can be concluded that the slope of the estimated flux error in terms of i_d , or the value of ($\frac{\Delta\tilde{\psi}_d}{\Delta I_d}$), has the opposite sign to the error value of the stator resistance ($-\tilde{R}_s$). It means that if the estimated resistance is lower than the actual resistance ($\hat{R}_s < R_s$), the resistance error value (\tilde{R}_s) is negative, and the value of ($\frac{\Delta\tilde{\psi}_d}{\Delta I_d}$) is positive, therefore, with a positive error, the value of the estimated flux in terms of i_d or ($\frac{\Delta\hat{\psi}_d}{\Delta I_d}$) is more than the real one. It can also be said that for positive values of \tilde{R}_s , the value of ($\frac{\Delta\hat{\psi}_d}{\Delta I_d}$) is less than the real one. This argument is also valid for the values of ($\frac{\Delta\hat{\psi}_q}{\Delta I_q}$) and ($\frac{\Delta\hat{\psi}_q}{\Delta I_d}$) which have the same sign as the error value of the stator resistance (\tilde{R}_s). However, in this study, we only use the third row of (13), as explained below.

The crucial point in this section is that, in the constant current of i_q , it is expected that ψ_q does not depend on the current i_d , thus the value of ($\frac{\Delta\hat{\psi}_q}{\Delta I_d}$) is expected to be equal to zero. However, according to (13), this value has the same sign as the error value of the stator resistance. It means, for $\tilde{R}_s > 0$, the value of ($\frac{\Delta\hat{\psi}_q}{\Delta I_d}$) is positive, so the value of ($\frac{\Delta\hat{\psi}_q}{\Delta I_d}$) is greater than zero and positive, and for $\tilde{R}_s < 0$, the value of ($\frac{\Delta\hat{\psi}_q}{\Delta I_d}$) and therefore ($\frac{\Delta\hat{\psi}_q}{\Delta I_d}$) is less than zero or negative. Therefore, by observing the sign of ($\frac{\Delta\hat{\psi}_q}{\Delta I_d}$), the sign of \tilde{R}_s can be found. From this, it is possible to determine if \hat{R}_s is greater or less than the actual resistance of the motor. In this paper, this behavior is used to estimate the stator resistance.

Before explaining the estimation algorithm in the simulation section, the effect of stator resistance mismatch on the estimated flux will be observed.

Table 1. Simulation Parameters

Parameter	Symbol	Value
Stator resistance	R_s	20mΩ
d -axis inductance	L_d	80μH
q -axis inductance	L_q	80μH
Mutual inductance between rotor and stator	M	3mH
Number of pole pairs	N_p	6

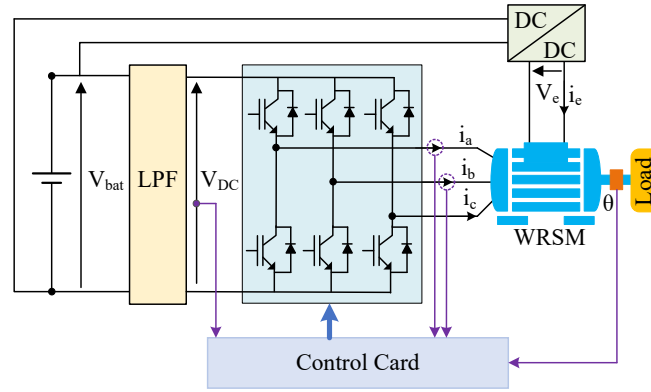


Figure 2. Schematic of the studied system.

4. Simulation and method explanation

To investigate the performances of the flux estimator and the effect of stator resistance mismatch, simulations are conducted for a WRSM with MATLAB Simulink. The WRSM studied is a low voltage and high current motor for automotive applications powered by a three-phase inverter and a 12-volt DC battery. The rotor also has a separate power supply that allows a higher degree of freedom for the control system. An input filter with a large capacitor is used to protect the battery from instantaneous currents and voltage peaks. Fig. 2 shows a schematic of this system, where the control card consists of a vector control with PI regulators for i_d and i_q . The parameters of the simulated model also are listed in TABLE 1.

4.1. Estimated flux

In these simulations, the method introduced in Fig.1 is applied to estimate the stator flux. The constant k in (5) is chosen as $k = 4$, and the lower limit of ω_c is considered equal to 1 for speeds close to zero, in order to avoid that the LPF time constant increases too much. In the first simulation, in a constant i_q , the estimated flux $\hat{\psi}_d$ is obtained as a function of the current i_d , and in a constant i_d , the estimated $\hat{\psi}_q$ is obtained in terms of i_q . Fig. 3 and Fig. 4 show the estimated flux $\hat{\psi}_d$ and $\hat{\psi}_q$ respectively, in three different cases: the blue one where the stator resistance is error-free, the red one where the initial resistance (or the resistance used in the flux estimator) is 50% higher than the actual value and the green one where the initial resistance is 50% lower than the actual value. Fig. 4 illustrates the estimated flux $\hat{\psi}_q$ in terms of i_q . As discussed before, the stator resistance error can cause an offset and a change in the slope. As it can be noticed in these figures, an error in the resistance value induces an error in the estimated flux. As discussed in the previous section, when the initial resistance is less than the actual value, the estimated flux has a positive offset, and when the initial resistance is greater than the actual value, the estimated flux has a negative offset. Also, as expected from (13), the slope of the diagrams could also contain an error.

Fig. 5 demonstrates the estimated flux $\hat{\psi}_q$ in terms of i_d . According to this figure, for an initial resistance lower than the actual value, the slope of this diagram is negative, and for a resistance higher than the actual value, the slope is positive. For the error-free case this value is equal to zero, in other words the flux $\hat{\psi}_q$ does not depend on the current i_d , which confirms the results obtained in equation (13). From the estimated flux $\hat{\psi}_q$ in terms of i_d , the error in the stator resistance can be detected. In another simulation, the flux $\hat{\psi}_q$ is estimated by applying a sinusoidal current at i_d for different values of \hat{R}_s . Fig. 6 illustrates the estimated flux $\hat{\psi}_q$ while i_q is constant, and there is a sinusoidal current injected into i_d , for different values \hat{R}_s . As shown in this figure, when the value of \hat{R}_s is bigger than the actual value, the estimated flux is in phase with i_d , which means, when i_d increases, the flux $\hat{\psi}_q$ also increases, and when i_d decreases, the estimated flux $\hat{\psi}_q$ also decreases. In the cases where the stator resistance is smaller than the actual value, it is observed that the flux $\hat{\psi}_q$ changes by 180 degrees of phase shift concerning i_d . In other words, the flux

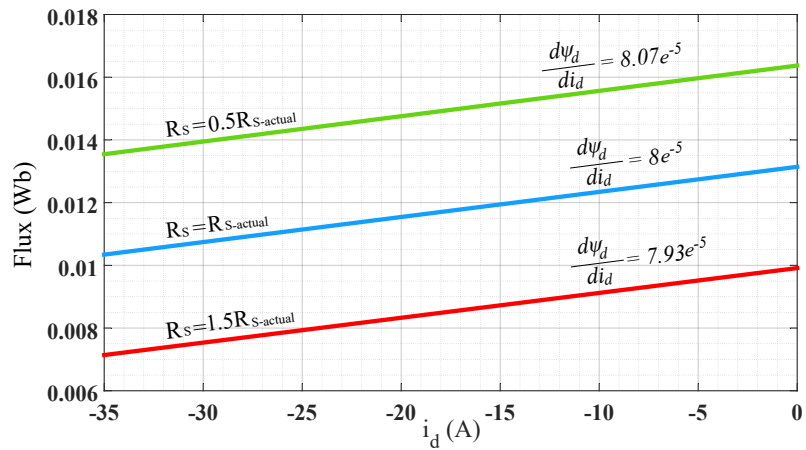


Figure 3. Simulation results: Flux ψ_d as a function of i_d in the case of R_s mismatch.

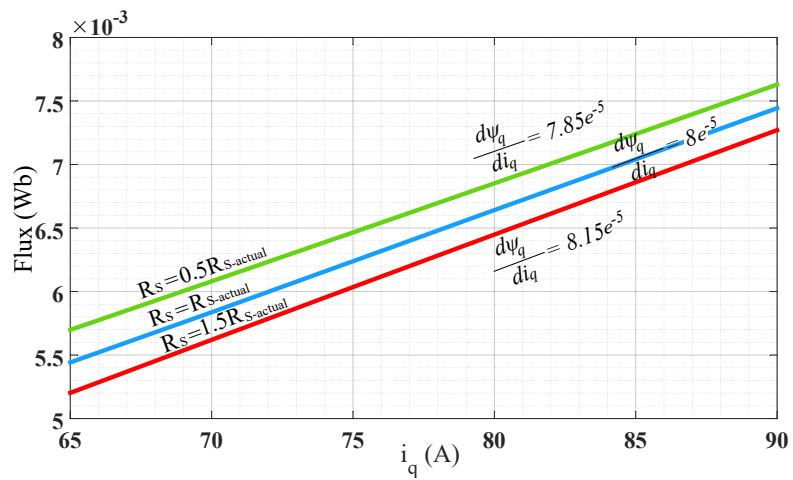


Figure 4. Simulation results: Flux ψ_q as a function of i_q in the case of R_s mismatch.

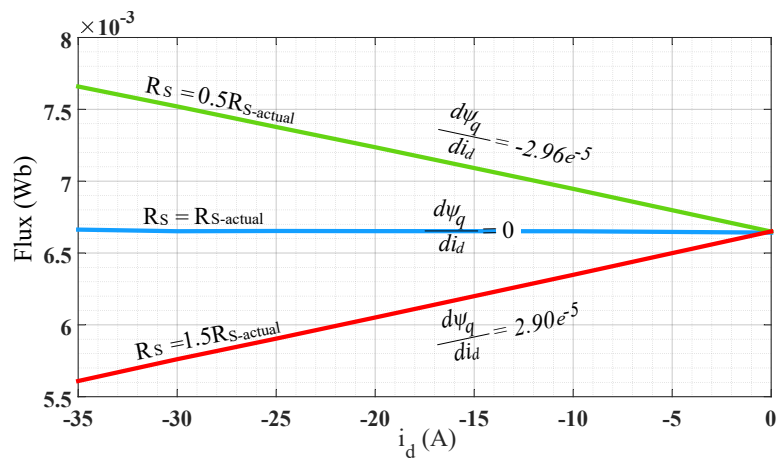


Figure 5. Simulation results: Flux ψ_q as a function of i_d in the case of R_s mismatch.

$\hat{\psi}_q$ decreases with the increase in i_d , and it increases with the decrease in i_d . When the resistance is error-free, as expected, the flux $\hat{\psi}_q$ does not depend on i_d , and despite the sinusoidal changes in i_d , the flux $\hat{\psi}_q$ is constant.

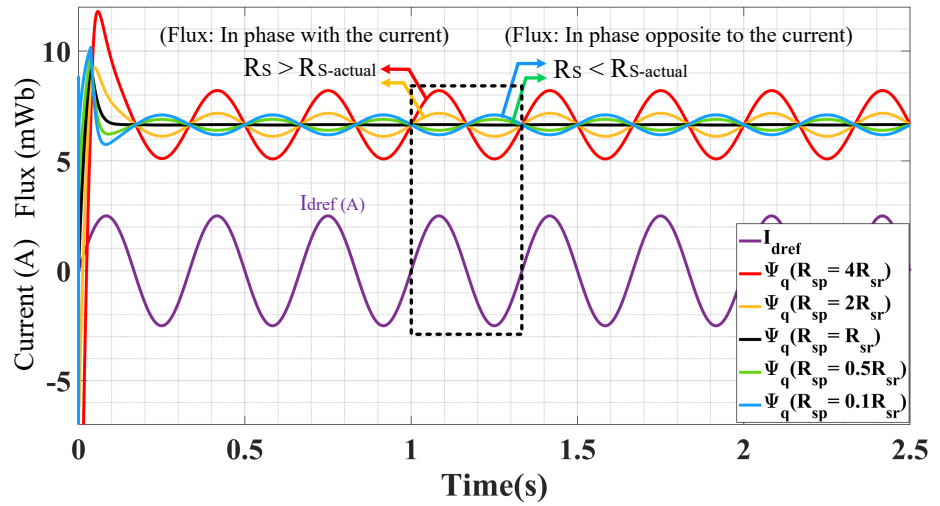


Figure 6. Simulation results: Flux ψ_q as a function of a sinusoidal variation of i_d in the case of R_s mismatch.

4.2. Estimation of Stator Resistance

In the previous subsection, it has been shown that in the case of stator resistance error, the estimated flux $\hat{\psi}_q$ varies as a function of i_d . Therefore, by observing the estimated flux $\hat{\psi}_q$ in terms of i_d , the stator resistance can be adjusted. The flowchart in Fig. 7 displays the resistance estimation algorithm. According to this flowchart, a sinusoidal signal is first applied to the d -axis current of the stator (i_d). Then, with the initial value of the stator resistance, the flux $\hat{\psi}_q$ is estimated. If the estimated flux $\hat{\psi}_q$ changes in proportion to i_d , the estimated resistance must be reduced. If $\hat{\psi}_q$ changes in opposite to i_d , the estimated resistance must be increased. The frequency of the iteration of this process is determined by the input flag which is explained later, and the process continues until the flux $\hat{\psi}_q$ no longer changes with changes in i_d .

To implement the proposed algorithm, it is required to choose the frequencies of the injected sinusoidal signal (f_{sin}) and the iteration time of the calculation block (or the sampling time). The selection of the frequency of the injected signal depends on the flux estimation rate. This frequency is limited by the LPF used to estimate the flux, and must be lower than the cutoff frequency of the LPF (ω_c), to ensure that the estimated flux is not affected by a drop in amplitude or a shift in phase. Selecting a sinusoidal signal frequency higher than the cutoff frequency of the filter may result in incorrect convergence of the estimator. To choose the sampling time, it should be considered that an acceptable number of samples are taken in a sinusoidal period, so a sampling time can be chosen to guarantee that $T_s < \frac{1}{20} T_{sin}$. The following simulations are performed at $i_d = 0$, $i_q = 90A$ and the rotor speed of $680rpm$. Considering the number of pole pairs $N_p = 6$, the electrical rotation frequency is equal to $\omega_e = 136\pi(rad.sec^{-1})$, and with $k = 4$, $\omega_c = 34\pi(rad.sec^{-1})$. The sinusoidal injected signal is selected as $i_{dref} = 2.5\sin(16\pi)$. Where $f_{sin} = 16\pi(rad.sec^{-1})$ is chosen less than $0.5\omega_c$. The amplitude also is chosen as $2.5A$, about 2% of the nominal current. In general, as the amplitude of the injected sinusoidal signal increases, the amplitude of the changes in the estimated flux increases, which can increase the rate of resistance estimation. However, a high current amplitude causes more losses. Choosing an amplitude of about 2% – 5% of the nominal current can lead to an acceptable estimation rate and also having few losses. The sampling frequency is also chosen equal to $T_s = 5ms$ about $\frac{1}{25} T_{sin}$. At each sampling, a flag is sent to the calculating block that leads the algorithm to an iteration. Fig. 8 summarizes the stator resistance estimation scheme of the proposed algorithm.

Now to observe the performance of the stator resistance estimator, other simulations are conducted for a WRSM in Matlab-simulink. In the first simulation, $i_{qref} = 90A$, and $i_{dref} = 2.5\sin(16\pi)$, and the initial value of the stator resistance is chosen $R_{sp} = 0.2\Omega$,

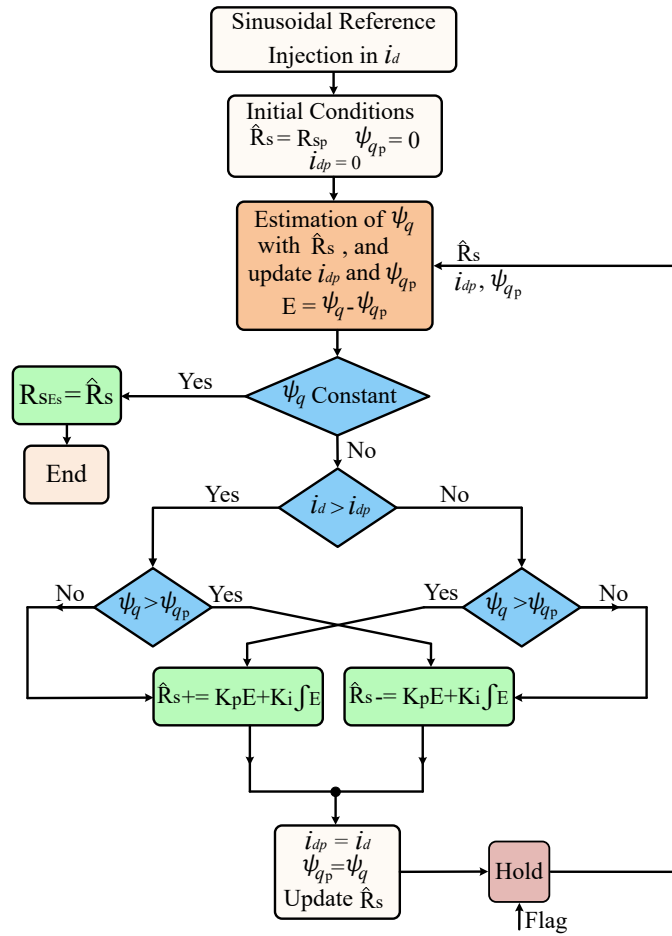


Figure 7. Algorithm of the proposed estimator. (subscript 'p' represents the variable in the previous time step).

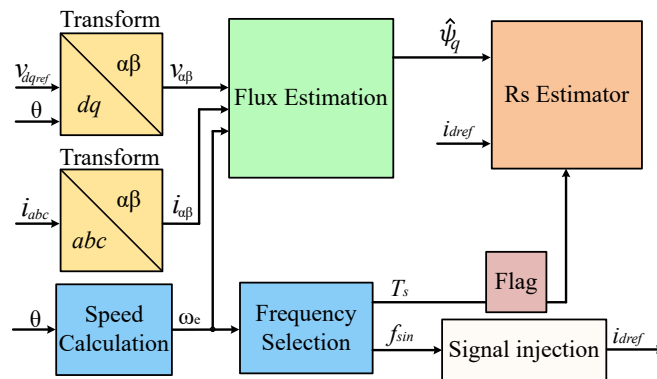


Figure 8. Stator resistance estimation scheme.

which is 10 times greater than its actual value. Fig. 9 shows the current i_d , the estimated flux $\hat{\psi}_q$, and the estimated resistance \hat{R}_s . The estimation method is applied at $t = 3s$ until $t = 5s$, when the resistance is estimated. At $t = 6s$ the real value of the resistance is changed to $R_s = 0.04\Omega$ and at $t = 7s$ the estimator is run again and the estimated resistance value converges towards the new resistance value. As it can be seen, the value of the stator resistance, despite a large error in the initial value, is correctly estimated in a fall time of $t_f = 0.375s$.

Fig. 10 also shows the estimation of stator resistance when the initial value is $R_{sp} = 0.002\Omega$,

294
295
296
297
298
299
300
301

which is 10 times less than its actual value. In this figure it can be seen that the estimation of the stator resistance behaves as expected. 302

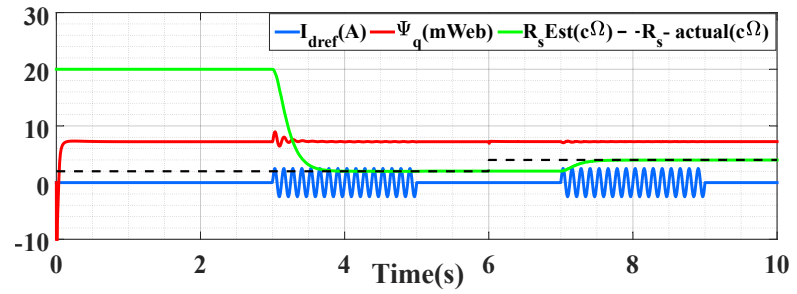


Figure 9. Simulation results: Estimated R_s , estimated flux ψ_q and with a sinusoidal signal injection on i_d .

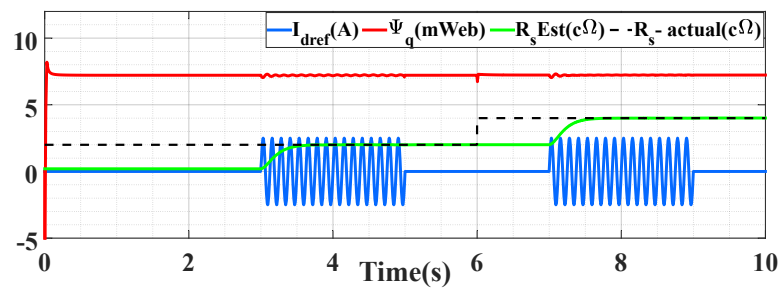


Figure 10. Simulation results: Estimated R_s , estimated flux ψ_q and with a sinusoidal signal injection on i_d .

4.3. Kalman Filter estimator 303

In this section, a comparison is made between the proposed estimator and the Kalman filter estimator. Kalman filter is a mathematical model that runs in parallel to the actual system and provides the estimation of the states of linear systems [35]. Fig. 11 shows the structure of an Extended Kalman Filter (EKF) observing the states of an actual system. 304
Using the system model of a WRSM, the state equations for the estimator can be presented as follows: 305

$$\begin{cases} \frac{di_d}{dt} = \frac{v_d}{L_d} - \frac{\hat{R}_s}{L_d} i_d + \frac{\omega_e L_q}{L_d} i_q \\ \frac{di_q}{dt} = \frac{v_q}{L_q} - \frac{\hat{R}_s}{L_q} i_q - \frac{\omega_e}{L_q} (L_d i_d + M i_e) \\ \frac{d\hat{R}_s}{dt} = 0 \end{cases} \quad (14) \quad 306$$

where, v_d and v_q are the voltages in the dq axes, i_e is the rotor excitation current and ω_e is the synchronous angular frequency. Also L_d and L_q are the stator inductance on the d and q axes and M is the mutual inductance between the rotor and the stator. This simulation 307
308
309
310
311
312
313

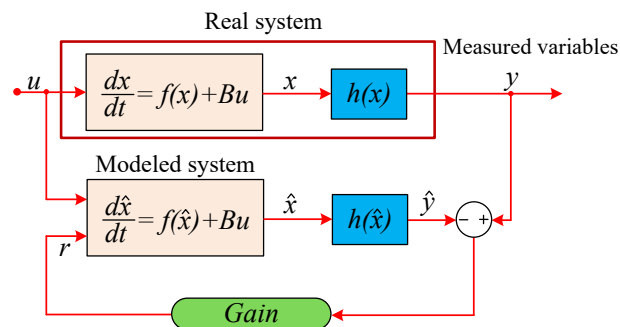


Figure 11. Structure of the Kalman filter estimator

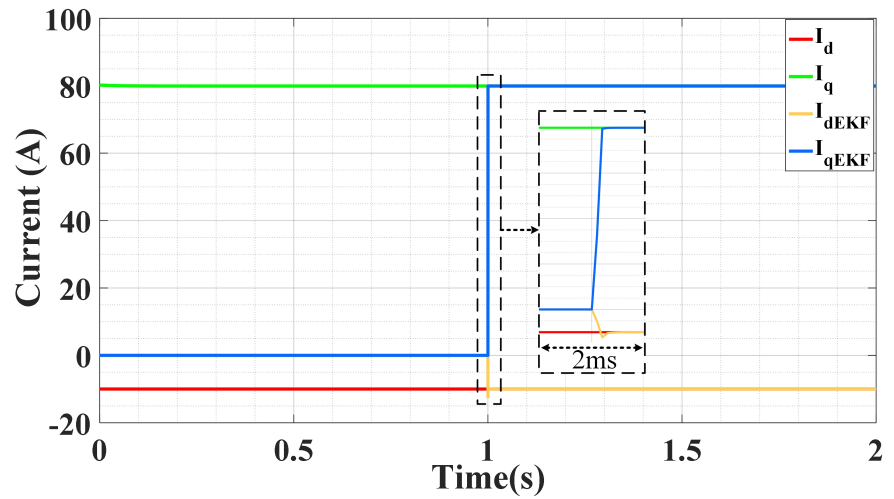


Figure 12. Simulation results: Measured and estimated currents by Kalman observer.

is performed at a constant current of $i_q = 80A$ and $i_d = -10A$. The estimated currents i_d 314
and i_q by the Kalman observer as well as the measured currents can be seen in Fig. 12. 315
The estimated resistance is also shown in Fig. 13. It is observed that the Kalman observer is 316
able to correctly estimate the stator resistance in a short time (less than $0.5ms$). However

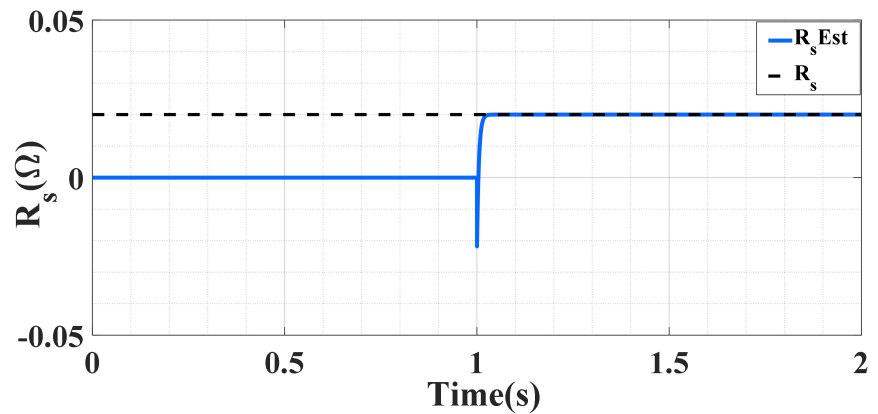


Figure 13. Simulation results: Actual resistance and estimated one by Kalman observer.

Kalman observer has two main drawbacks: the first problem is a high computational load, 317
and the second one, like the other model-based observers, is that it depends on the model 318
parameters. To estimate the stator resistance, the values of the motor parameters such as 319
 L_d , L_q and M need to be specified in the EKF design, while with the proposed method, 320
those parameters are not needed. In model based observers, an error in each parameter 321
leads to an error in the estimated parameter. To observe the effect of motor parameters 322
error on estimated resistance, the motor parameters are given to the Kalman observer with 323
some errors. Fig. 14 illustrates the estimated resistance while there are errors in the other 324
parameters. Fig. 14 illustrates the estimated resistance while there are errors in the other 325
parameters. 326

In Fig. 14, it can be seen that if only L_d or L_q have 50% error, the resistance value of 327
 R_s is estimated with an error of 8.5% and 15% respectively. If both L_d and L_q have a 50% 328
error, the error is greater (about 50%). This error increases when the mutual inductance 329
 M has an error, because as it can be seen in TABLE 1, its value is much higher than the dq 330
inductances. In this figure the red diagram shows the estimated resistance while M is 50% 331
lower than the actual value, and the purple diagram shows the estimated resistance while 332
 M is 50% greater than the actual value, at which the errors correspond to 50% and 150% 333
respectively. These results show that despite the high speed of the Kalman estimator to 334

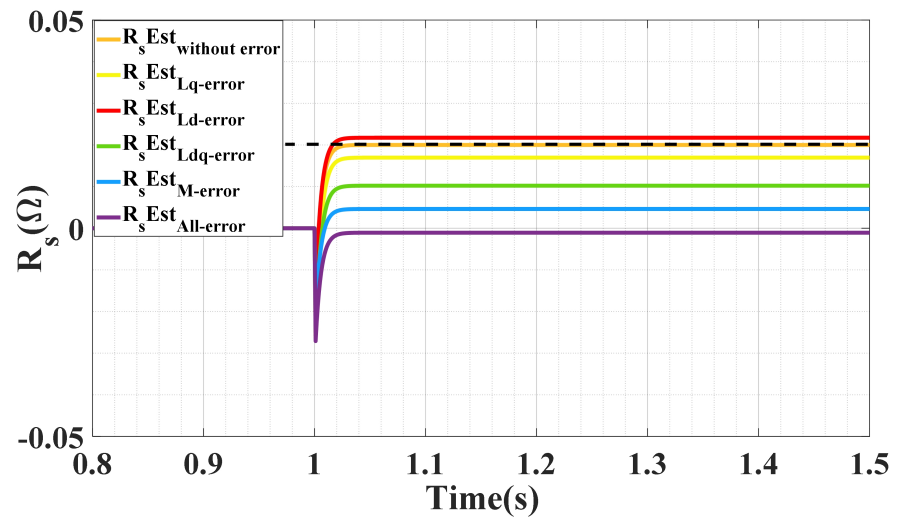


Figure 14. Simulation results: Estimated resistance by Kalman observer when errors in the parameters are added.

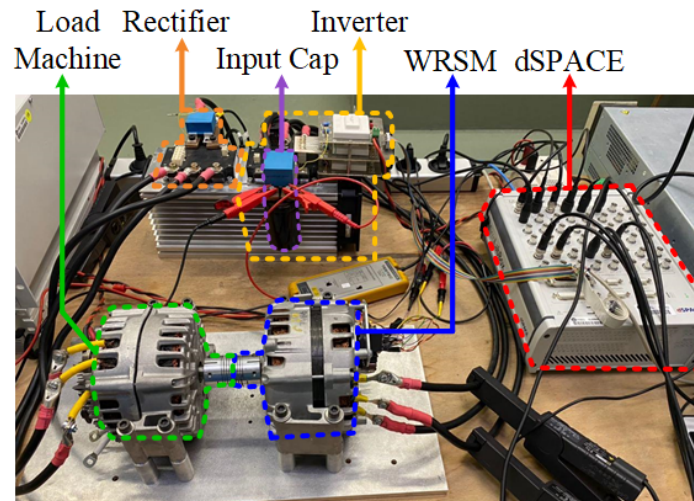


Figure 15. Experimental test bench.

estimate the stator resistance, if the other parameters of the model contain an error, the estimated resistance will also have an error which can be significant in certain cases as it can be seen in Fig. 14.

5. Experimental results

In order to verify the proposed estimator, experimental tests have been carried out on a WRSM. The prototype platform is shown in Fig. 15. The WRSM under study is designed by Valeo for mild-hybrid applications for automotive industry with 12V rated voltage, 1.5kW rated power and excitation current of rotor up to 8A. The experimental setup consists of two WRSMs, the first machine is controlled and its stator resistance is estimated and the other is used as a load for the first machine. A dSPACE MicroLabBox is used to control the system and sends the switching signals to a three phase inverter with a frequency of 10kHz. A 12 volt DC power supply is used as the input source of the inverter to emulate a car battery. The rotor excitation winding is also powered by a controllable DC voltage source.

5.1. Flux estimation

In the first test, the effect of a resistance mismatch on the estimated flux will be studied. To do so, with a current reference of $i_q = 35A$, a sinusoidal current is applied to i_d and the flux $\hat{\psi}_q$ is estimated.

In this test, a sinusoidal current is applied to i_d and the flux $\hat{\psi}_q$ is estimated while the value of the stator resistance in the equations of the flux estimator is first set to a value 50% lower than its actual value, then it is set equal to its real value, then it is fixed to a value 50% higher than its real value.

Fig. 16 shows the current i_d and the estimated flux $\hat{\psi}_q$. In this figure, as in the simulation results, it is observed that at the beginning, when the set value of R_s is lower than its real value, the current i_d and the flux $\hat{\psi}_q$ have a phase difference of 180 degrees, so the flux $\hat{\psi}_q$ decreases when i_d increases and it increases when i_d decreases. Then, when the fixed value of R_s is equal to its real value, $\hat{\psi}_q$ is almost constant and stable. Finally, when the set value of the resistance is greater than its real value, the current i_d and the flux $\hat{\psi}_q$ are in phase.

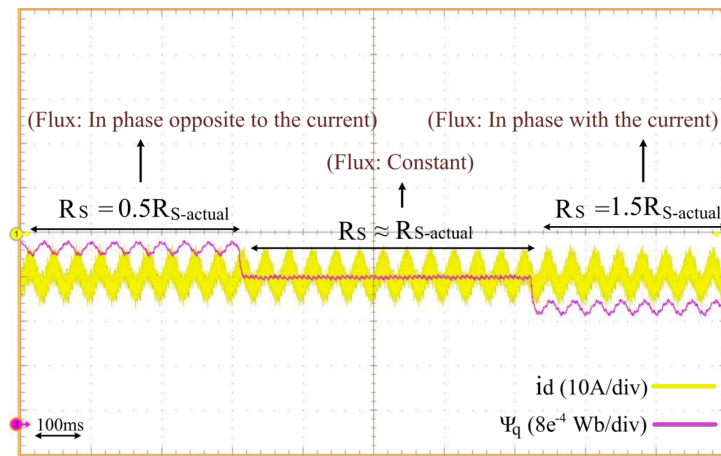


Figure 16. Estimated flux with a sinusoidal signal injection on i_d for different value of R_s .

5.2. Stator resistance estimation

In the next test the resistance estimation algorithm is implemented. In this experiment, $i_q = 35A$, and for the sinusoidal signal injected into i_d , the frequency of the sinusoidal wave is 16π ($rad.s^{-1}$) and the amplitude is equal to $5A$ (about 4% of the nominal current). In the first test the initial resistance value is considered $2m\Omega$. The sinusoidal signal is injected into i_d , and the estimation algorithm is executed. Fig. 17 illustrates the result of this estimation. As shown in Fig. 17, the estimated flux first oscillates sinusoidally with a phase shift of 180 degrees with i_d . Then, by starting the resistance estimation algorithm, the amplitude of the estimated flux oscillation is decreased and the estimated resistance converges towards $27.2m\Omega$.

This experiment is repeated under the same conditions, but this time the initial value of the stator resistance is chosen as $200m\Omega$. The result of this estimation is also illustrated in Fig. 18. As it is seen, first the estimated flux has oscillations in phase with i_d . Then, after starting the estimation, the oscillation in the estimated flux is reduced, and the estimated resistance converges to $27.2m\Omega$.

5.3. The effect of sudden change in load

To investigate how the estimator responds to a sudden change in load level and shaft speed, another experiment is performed. In this test, the motor currents (i_d and i_q) are kept constant and the rotor speed varies with the output load. As mentioned earlier, a second machine is connected to the studied machine as an output load. The second machine works as a generator and supplies a resistive load. In this test, to make a sudden change in the motor load, the resistive load connected to the generator suddenly changes. Fig. 19 shows

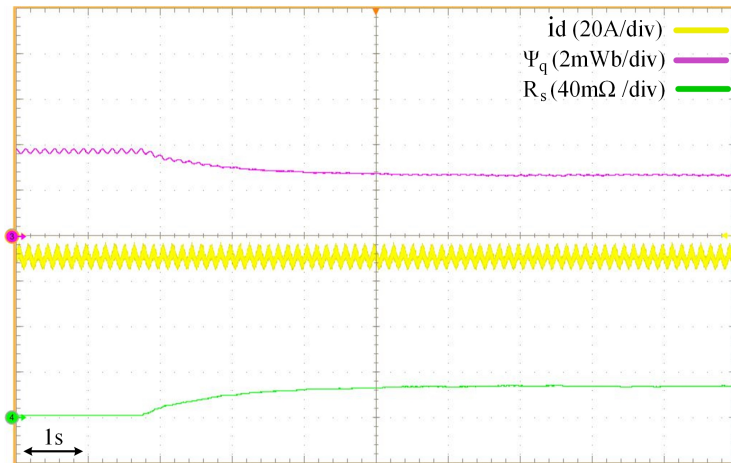


Figure 17. Estimated resistance when the initial value is about 10 times smaller than the actual value.

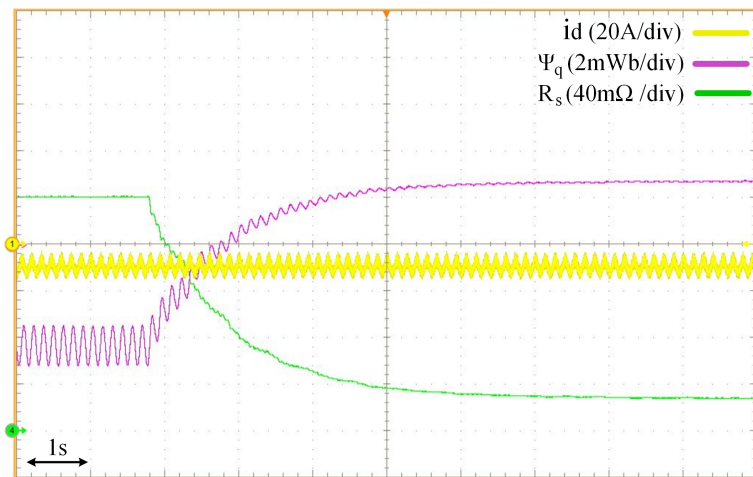


Figure 18. Estimated resistance when the initial value is about 10 times bigger than the actual value.

the stator resistance estimation during the load changes. In this figure, it is observed that after a sudden change in output load, the estimated resistance remains stable.

5.4. Estimation of resistance by Kalman observer

In this part, to compare and validate the proposed estimator, a Kalman filter observer is applied to estimate the stator resistance. In this test, the stator currents are equal to $i_d = 0$ and $i_q = 35$. Fig. 20 illustrates the resistance estimated with the Kalman observer which converges to $28m\Omega$. Fig. 21 also shows the estimated resistance in the case of error in the motor parameters. It can be seen, like the simulation part, for the error of 50% on L_d or L_q the estimated resistance faces a small error (5.7%). This error increases with a mismatch in the mutual inductance M , the red diagram in this figure shows the estimated resistance while M is about 50% lower than the actual value (which leads to an error of 89% in the estimated resistance), and the purple diagram shows the estimated resistance while M is about 50% bigger than the actual value (which causes an error of 135% in the estimated resistance). The results observed in this section demonstrated the sensitivity of model-based estimators and it was observed that in this type of estimators, an error in one of the model parameters can lead to a significant error in the estimated parameter. Though, the proposed estimator is completely independent of the model parameters.

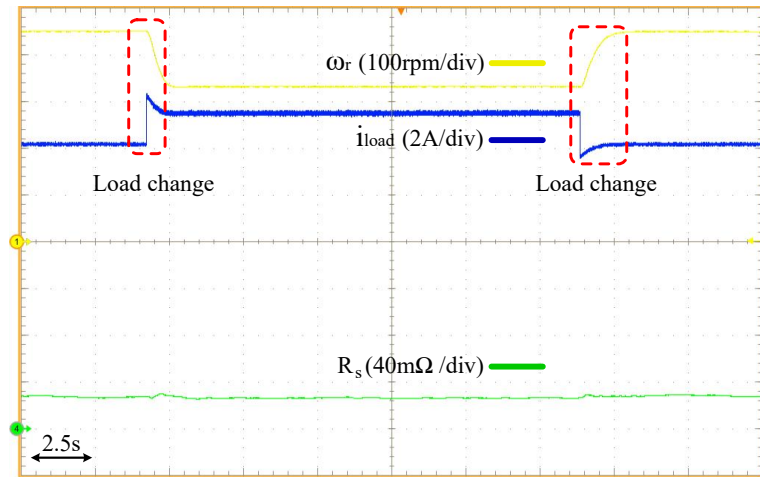


Figure 19. Estimated stator resistance during load change.

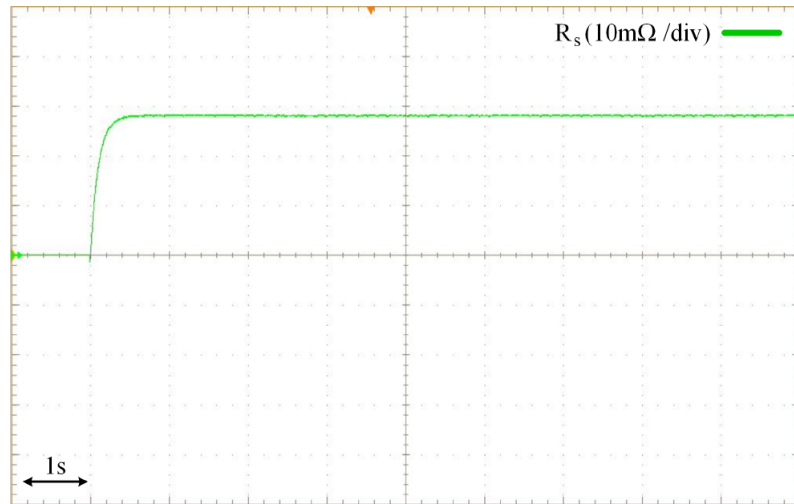


Figure 20. Experimental estimated resistance with Kalman observer.

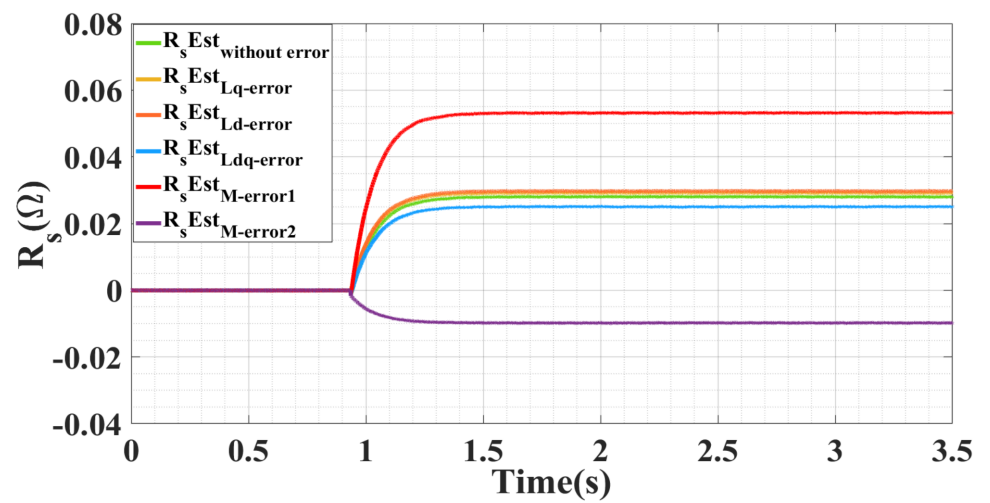


Figure 21. Experimental estimated resistance with Kalman observer while there are errors in the parameters.

6. Conclusions

In this paper, a new method based on low frequency signal injection has been proposed to estimate the stator resistance. This technique is based on the phase difference between the injected sinusoidal current and the estimated flux variations. In this method, a low frequency sinusoidal current is injected into the d axis of the stator and during this time the stator flux is estimated. It was shown that by injecting a low frequency sinusoidal signal into the stator d -axis, in case of stator resistance mismatch, the estimated flux of the q -axis gets sinusoidal variation, and the phase difference between the injected sinusoidal signal and the sinusoidal variation of the estimated flux is related to the value of estimated stator resistance. This phase difference was used to adjust the stator resistance. The proposed method provides a simple, parameter-free technique for estimating stator resistance without the need for the parameters of the machine model, such as stator and rotor inductances or the rotor flux linkage.

The simulation work, first, showed the effect of a stator resistance mismatch on the estimated flux, which confirmed the presented equations and discussion. Then, the implementation of the proposed estimator showed that the estimated resistance converges to the actual value.

A comparison with the Kalman observer also illustrated the advantage of the proposed estimator. The results demonstrated the sensitivity of the model-based estimators and it was observed that in this type of estimators, an error in one of the model parameters can lead to a significant error in the estimated parameter (up to a few tens of percent error). While the proposed estimator is completely independent of the model parameters. However, the Kalman observer can estimate the stator resistance in a short time (less than 0.5 ms), while the proposed method cannot be as fast due to the nature of the low-frequency injection method which can take few seconds.

Finally, the performances of the estimator was validated on a test bench. The experimental results as well as the simulation results have clearly shown that even in the case where the initial value of the resistance is far from the real value, the proposed method can converge and estimate the value of stator resistance precisely.

References

1. Tang, J.; Yang, Y.; Blaabjerg, F.; Chen, J.; Diao, L.; Liu, Z. Parameter identification of inverter-fed induction motors: A review. *Energies* **2018**, *11*, 2194.
2. Mahfoud, S.; Derouich, A.; El Ouanjli, N.; Mossa, M.A.; Bhaskar, M.S.; Lan, N.K.; Quynh, N.V. **A New Robust Direct Torque Control Based on a Genetic Algorithm for a Doubly-Fed Induction Motor: Experimental Validation.** *Energies* **2022**, *15*, 5384.
3. Corne, A.; Yang, N.; Martin, J.P.; Nahid-Mobarakeh, B.; Pierfederici, S. Nonlinear estimation of stator currents in a wound rotor synchronous machine. *IEEE Transactions on Industry Applications* **2018**, *54*, 3858–3867.
4. Haghgooei, P.; Corne, A.; Jamshidpour, E.; Takorabet, N.; Khaburi, D.A.; Nahid-Mobarakeh, B. **Current sensorless control for a wound rotor synchronous machine based on flux linkage model.** *IEEE Journal of Emerging and Selected Topics in Power Electronics* **2021**, *10*, 4576–4586.
5. Zerdali, E. Adaptive extended Kalman filter for speed-sensorless control of induction motors. *IEEE Transactions on Energy Conversion* **2018**, *34*, 789–800.
6. Ameid, T.; Menacer, A.; Talhaoui, H.; Harzelli, I. Rotor resistance estimation using Extended Kalman filter and spectral analysis for rotor bar fault diagnosis of sensorless vector control induction motor. *Measurement* **2017**, *111*, 243–259.
7. Liu, K.; Feng, J.; Guo, S.; Xiao, L.; Zhu, Z.Q. Identification of flux linkage map of permanent magnet synchronous machines under uncertain circuit resistance and inverter nonlinearity. *IEEE Transactions on Industrial Informatics* **2017**, *14*, 556–568.
8. Saadaoui, O.; Khlaief, A.; Abassi, M.; Tlili, I.; Chaari, A.; Boussak, M. A new full-order sliding mode observer based rotor speed and stator resistance estimation for sensorless vector controlled PMSM drives. *Asian Journal of Control* **2019**, *21*, 1318–1327.
9. Hinkkanen, M.; Harnefors, L.; Luomi, J. Reduced-order flux observers with stator-resistance adaptation for speed-sensorless induction motor drives. *IEEE Transactions on Power Electronics* **2009**, *25*, 1173–1183.

10. Saejia, M.; Sangwongwanich, S. Averaging analysis approach for stability analysis of speed-sensorless induction motor drives with stator resistance estimation. *IEEE Transactions on Industrial Electronics* **2006**, *53*, 162–177. 457
458
11. Abdelrahem, M.; Hackl, C.M.; Rodríguez, J.; Kennel, R. Model reference adaptive system with finite-set for encoderless control of PMSGs in micro-grid systems. *Energies* **2020**, *13*, 4844. 460
461
12. Bednarz, S.A.; Dybkowski, M. Estimation of the Induction Motor Stator and Rotor Resistance Using Active and Reactive Power Based Model Reference Adaptive System Estimator. *Applied Sciences* **2019**, *9*, 5145. 462
463
464
13. Holakooie, M.H.; Ojaghi, M.; Taheri, A. Direct torque control of six-phase induction motor with a novel MRAS-based stator resistance estimator. *IEEE Transactions on Industrial Electronics* **2018**, *65*, 7685–7696. 465
466
467
14. Khan, Y.A.; Verma, V. A novel method of estimating stator resistance for an F-MRAS based speed sensorless vector controlled switched reluctance motor drive. In Proceedings of the 2019 54th International Universities Power Engineering Conference (UPEC). IEEE, 2019, pp. 1–6. 468
469
470
15. Sivakumar, M.; Thanakodi, T.; Selvam, N.P. Comparative Analysis of Stator Resistance Estimators in DTC-CSI Fed IM Drive. *International Journal of Applied Engineering Research* **2018**, *13*, 12364–12372. 471
472
473
16. Rashed, M.; MacConnell, P.F.; Stronach, A.F.; Acarnley, P. Sensorless indirect-rotor-field-orientation speed control of a permanent-magnet synchronous motor with stator-resistance estimation. *IEEE Transactions on Industrial Electronics* **2007**, *54*, 1664–1675. 474
475
476
17. Heidari, H.; Rassolkin, A.; Holakooie, M.H.; Vaimann, T.; Kallaste, A.; Belahcen, A.; et al. A parallel estimation system of stator resistance and rotor speed for active disturbance rejection control of six-phase induction motor. *Energies* **2020**, *13*, 1121. 477
478
479
18. Vazifedan, M.; Zarchi, H.A. A Stator Resistance Estimation Algorithm For Sensorless Dual Stator Winding Induction Machine Drive Using Model Reference Adaptive System. In Proceedings of the 11th Power Electronics, Drive Systems, and Technologies Conference (PEDSTC). IEEE, 2020, pp. 1–7. 480
481
482
483
19. Khadar, S.; Kouzou, A.; Benguesmia, H. Fuzzy stator resistance estimator of induction motor fed by a three levels NPC inverter controlled by direct torque control. In Proceedings of the 2018 International Conference on Applied Smart Systems (ICASS). IEEE, 2018, pp. 1–7. 484
485
486
20. Luo, C.; Wang, B.; Yu, Y.; Chen, C.; Huo, Z.; Xu, D. Decoupled stator resistance estimation for speed-sensorless induction motor drives considering speed and load torque variations. *IEEE Journal of Emerging and Selected Topics in Power Electronics* **2019**, *8*, 1193–1207. 487
488
489
21. Liang, D.; Li, J.; Qu, R. Sensorless control of permanent magnet synchronous machine based on second-order sliding-mode observer with online resistance estimation. *IEEE Transactions on Industry Applications* **2017**, *53*, 3672–3682. 490
491
492
22. Haghgooei, P.; Jamshidpour, E.; Takorabet, N.; Arab-khaburi, D.; Nahid-Mobarakeh, B. Magnetic Model Identification of Wound Rotor Synchronous Machine Using a Novel Flux Estimator. *IEEE Transactions on Industry Applications* **2021**. 493
494
495
23. Zhang, P.; Lu, B.; Habetler, T.G. A remote and sensorless stator winding resistance estimation method for thermal protection of soft-starter-connected induction machines. *IEEE Transactions on Industrial Electronics* **2008**, *55*, 3611–3618. 496
497
498
24. Lazcano, U.; Poza, J.; Garramiola, F.; Rivera, C.A.; Iturbe, I. **Double Dead-Time Signal Injection Strategy for Stator Resistance Estimation of Induction Machines.** *Applied Sciences* **2022**, *12*, 8812. 499
500
25. Baneira, F.; Asiminoaei, L.; Doval-Gandoy, J.; Delpino, H.A.M.; Yepes, A.G.; Godbersen, J. Estimation method of stator winding resistance for induction motor drives based on DC-signal injection suitable for low inertia. *IEEE Transactions on Power Electronics* **2018**, *34*, 5646–5654. 501
502
503
26. Underwood, S.J.; Husain, I. Online parameter estimation and adaptive control of permanent-magnet synchronous machines. *IEEE Transactions on Industrial Electronics* **2009**, *57*, 2435–2443. 504
505
27. Reigosa, D.D.; Fernandez, D.; Zhu, Z.Q.; Briz, F. PMSM magnetization state estimation based on stator-reflected PM resistance using high-frequency signal injection. *IEEE Transactions on Industry Applications* **2015**, *51*, 3800–3810. 506
507
508
28. Baghli, L.; Al-Rouh, I.; Rezzoug, A. **Signal analysis and identification for induction motor sensorless control.** *Control engineering practice* **2006**, *14*, 1313–1324. 509
510
29. Boroujeni, S.T.; Takorabet, N.; Mezani, S.; Lubin, T.; Haghgooei, P. Using and enhancing the cogging torque of PM machines in valve positioning applications. *IET Electric Power Applications* **2020**. 511
512
513

30. Liu, K.; Zhu, Z.Q.; Stone, D.A. Parameter estimation for condition monitoring of PMSM stator winding and rotor permanent magnets. *IEEE Transactions on Industrial Electronics* **2013**, *60*, 5902–5913. 514
515
31. Wu, X.; Feng, Y.; Liu, X.; Huang, S.; Yuan, X.; Gao, J.; Zheng, J. Initial rotor position detection for sensorless interior PMSM with square-wave voltage injection. *IEEE Transactions on Magnetics* **2017**, *53*, 1–4. 517
518
519
32. Zhang, X.; Li, H.; Yang, S.; Ma, M. Improved initial rotor position estimation for PMSM drives based on HF pulsating voltage signal injection. *IEEE Transactions on Industrial Electronics* **2017**, *65*, 4702–4713. 520
521
522
33. Idris, N.R.N.; Yatim, A.H.M. An improved stator flux estimation in steady-state operation for direct torque control of induction machines. *IEEE Transactions on Industry Applications* **2002**, *38*, 110–116. 523
524
525
34. Shin, M.H.; Hyun, D.S.; Cho, S.B.; Choe, S.Y. An improved stator flux estimation for speed sensorless stator flux orientation control of induction motors. *IEEE Transactions on Power Electronics* **2000**, *15*, 312–318. 526
527
528
35. Yildiz, R.; Barut, M.; Zerdali, E. A comprehensive comparison of extended and unscented Kalman filters for speed-sensorless control applications of induction motors. *IEEE Transactions on Industrial Informatics* **2020**, *16*, 6423–6432. 529
530
531

Disclaimer/Publisher’s Note: The statements, opinions and data contained in all publications are solely those of the individual author(s) and contributor(s) and not of MDPI and/or the editor(s). MDPI and/or the editor(s) disclaim responsibility for any injury to people or property resulting from any ideas, methods, instructions or products referred to in the content. 532
533
534
535